Complexes of 2,2′-biphenol with ruthenium(II), molybdenum(V), tungsten(V) and tungsten(VI): structures, electrochemistry and spectroscopy

Rebecca H. Laye, Zöe R. Bell and Michael D. Ward*

School of Chemistry, University of Bristol, Cantock's Close, Bristol, UK BS8 1TS. E-mail: mike.ward@bristol.ac.uk; Fax: (+44) 117 9290509

Received (in London, UK) 3rd December 2002, Accepted 5th February 2003
First published as an Advance Article on the web 25th February 2003

Complexes of the potentially bidentate ligand 2,2′-biphenol (H_2biph) have been prepared and studied by electrochemical and UV/Vis/NIR spectroelectrochemical methods. The complexes studied are [(Tp*)M(O)(biph)] [M = Mo, W; Tp* = hydrotris(3,5-dimethylpyrazolyl)borate], [W(biph)$_3$], [Cl_6W_2(biph)$_3$] and [Ru(bpy)$_2$(biph)], and all have been structurally characterised. [(Tp*)M(O)(biph)] (M = Mo, W) both undergo reversible M(IV)/M(V) couples at negative potentials, with the redox potential for the W(IV)/W(V) couple being 580 mV more negative than that of the Mo(IV)/Mo(V) couple; the redox potentials are similar to those which occur in the complexes [(Tp*)M(O)(OC_6H_5)$_2$] with two monodentate phenolate ligands. The structure of [W(biph)$_3$] is essentially octahedral but with a distortion towards trigonal prismatic; the complex undergoes two metal-centred redox processes, W(IV)/W(V) and W(V)/W(VI) which were characterised spectroelectrochemically. An unexpected new W(VI) complex [Cl_6W_2(biph)$_3$] has the structure [{WCl_3(biph)}$_2$(μ-biph)], in which each W(VI) centre has a terminal chelating biphenolate ligand, and other highly twisted biphenolate ligand acts as a bis-monodentate bridge spanning the two W(VI) centres. [Cl_6W_2(biph)$_3$] undergoes two successive W(V)/W(VI) redox processes at negative potentials, with a separation of 170 mV indicating a through-space Coulombic interaction between the metal centres; spectroelectrochemistry showed no evidence of an inter-valence charge-transfer band in the mixed-valence W(V)–W(VI) state. [Ru(bpy)$_2$(biph)] has a Ru(II)/Ru(III) couple at a potential very similar to related ruthenium complexes with a (pyridine)$_4$(phenolate)$_2$ donor set.

Introduction

In this paper we describe the syntheses, crystal structures, spectroscopic and electrochemical properties of a series of complexes of the bidentate chelating ligand 2,2′-biphenol with W(V), W(VI), Mo(V) and Ru(II). 1,1′-Bis(2-aryloxides) such as binaphthol have been extensively used to generate asymmetric induction in homogeneous catalysis.[1] Further, addition of bulky substituents at the C3 and C3′ positions influences the structures and reactivities of metal complexes by sterically crowding the metal coordination environment.[2,3] Complexes of the unsubstituted parent ligand 2,2′-biphenol however are relatively rare.[3,4] 2,2′-Biphenols usually appear to coordinate as bidentate chelates, whose 7-membered chelate ring induces the characteristic twist between the two phenyl rings on coordination;[2,3] however a bridging coordination mode (in which one phenolate residue spans two metal centres) has also been observed in polynuclear manganese clusters.[3b]

The complexes described and structurally characterised in this paper are [(Tp*)M(O)(biph)$_2$] (M = Mo, W) which contain oxo–Mo(V) or oxo–W(V) units; the (previously described) complex [W(biph)$_3$],[4] and an unexpected dinuclear complex [Cl_6W_2(biph)$_3$] in which the biphenolate ligands exhibit two different coordination modes; and finally the complex [Ru(bpy)$_2$(biph)].

Results and discussion

Oxo–Mo(V) and oxo–W(V) complexes

In the oxo–M(V) complexes [(Tp*)M(O)Cl_2] (M = Mo, W), one or both of the chloride ligands can be replaced by other anionic ligands such as phenolates,[5] a property which has been exploited in the study of extensive series of dinuclear complexes containing 4,4′-biphenolate bridging ligands.[6] The complexes [(Tp*)M(O)(biph)] were prepared by first refluxing 2,2′-biphenol in pyridine with sodium hydride to deprotonate the phenolic groups, and then adding either the molybdenum or tungsten precursors [(Tp*)OMCl_2] and continuing the reflux. The formation of the molybdenum complex was much faster, and much higher yielding, than that of the tungsten complex.

[(Tp*)Mo(O)(biph)] was isolated as a dark green solid. The EI mass spectrum shows clusters of peaks with the correct isotopic pattern at m/z 595 and 498 corresponding to the molecular ion, and loss of a pyrazolyl ring from the molecular ion, respectively. Infra-red spectroscopy (solid state) shows bands associated with the B–H, Tp* and Mo=O fragments at 2541, 1543 and 941 cm^{-1} respectively. The frequency of the MoO vibration is significantly altered from that of the starting material [(Tp*)Mo(O)Cl_2] (960 cm^{-1}). This indicates a weakening of the Mo=O bond, presumably because the phenolates are acting here as stronger electron donors than chlorides: the increase in electron density at the metal will inhibit $O^{2-} \rightarrow$ Mo π-donation, thereby weakening the bond. The isotropic EPR spectrum of [(Tp*)Mo(O)(biph)] in CH_2Cl_2 solution shows the typical 'singlet plus sextet' pattern at $g = 1.933$ characteristic of mononuclear molybdenum complexes, arising from a mixture of Mo isotopes with $I = 0$ (singlet) and $I = 5/2$ (sextet, with $A_{Mo} = 50$ Gauss).[5,6]

X-Ray quality crystals of [(Tp*)Mo(O)(biph)] were grown from a $CHCl_3$/heptane mixture as dark green blocks. The crystal structure is illustrated in Fig. 1 (see also Table 1).

 DOI: 10.1039/b211997h

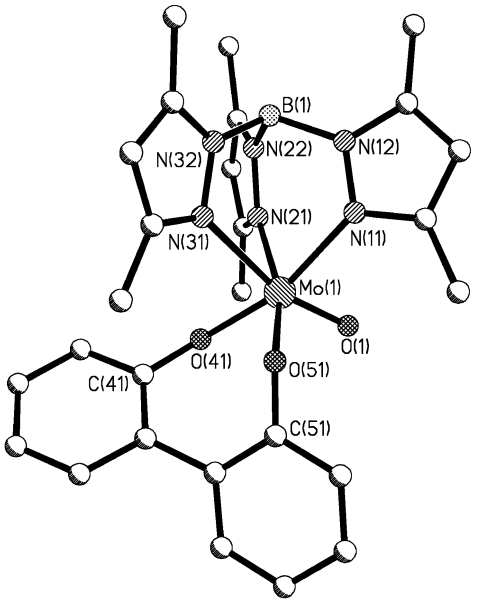

Fig. 1 Molecular structure of [(Tp*)Mo(O)(biph)].

The coordination geometry at the metal centre is the expected distorted octahedron. The Mo(1)–O(41) and Mo(1)–O(51) distances of 1.9281(18) and 1.9608(18) Å respectively are comparable to average Mo–O(phenolato) bond distance of 1.940 Å in other phenolate–Mo(V) complexes,[6] but are slightly shorter than the Mo(V)–O(catecholate) bond distances of *ca.* 1.99 Å in [(Tp*)Mo(O)(Cl_4cat)].[7] The bond distances O(41)–C(41) and O(51)–C(51) are 1.347(3) Å and 1.374(3) Å respectively, and are consistent with single C–O bond character.[8] The Mo–N distances are markedly inequivalent at 2.162(2), 2.200(2) and 2.348(2) Å, with the longest being the one *trans* to the π-donor oxo-ligand. There is, as usual, a significant twist in the biphenolate ligand with the torsion angle between the two phenyl rings being 45.1°.

The cyclic voltammogram of [(Tp*)Mo(O)(biph)] in acetonitrile shows a single symmetric wave at $E_{1/2} = -1.38$ V *vs.* $FeCp_2^{0/+}$ ($\Delta E_p = 122$ mV), assigned as a chemically reversible Mo(V)/(IV) couple. There are also two irreversible processes at

Table 1 Selected bond distances (Å) and angles (°) for [(Tp*)Mo(O)(biph)]

Mo(1)–O(1)	1.6822(18)
Mo(1)–O(41)	1.9281(18)
Mo(1)–O(51)	1.9608(18)
Mo(1)–N(21)	2.162(2)
Mo(1)–N(11)	2.200(2)
Mo(1)–N(31)	2.348(2)
O(1)–Mo(1)–O(41)	104.85(8)
O(1)–Mo(1)–O(51)	99.94(8)
O(41)–Mo(1)–O(51)	88.09(8)
O(1)–Mo(1)–N(21)	94.73(9)
O(41)–Mo(1)–N(21)	83.94(8)
O(51)–Mo(1)–N(21)	164.70(8)
O(1)–Mo(1)–N(11)	87.75(9)
O(41)–Mo(1)–N(11)	164.76(8)
O(51)–Mo(1)–N(11)	98.28(8)
N(21)–Mo(1)–N(11)	86.55(8)
O(1)–Mo(1)–N(31)	163.79(8)
O(41)–Mo(1)–N(31)	90.38(8)
O(51)–Mo(1)–N(31)	85.86(8)
N(21)–Mo(1)–N(31)	81.17(8)
N(11)–Mo(1)–N(31)	76.38(8)
C(41)–O(41)–Mo(1)	137.76(17)
C(51)–O(51)–Mo(1)	121.78(15)

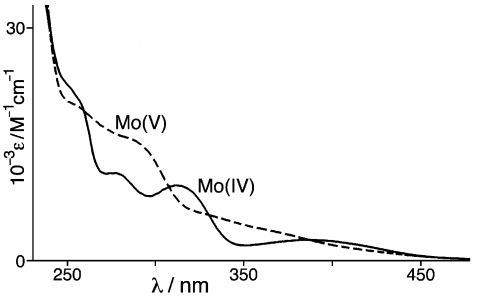

Fig. 2 Electronic spectra of $[(Tp^*)Mo(O)(biph)]^{n-}$ ($n = 0$, dotted line; $n = 1$, solid line) from an OTTLE experiment in MeCN at 243 K.

$E_{1/2} = +0.79$ and $+1.06$ V which could be either phenolate-based, or metal-based Mo(V)/Mo(VI) processes; the fact that the first of these moves to a much more negative potential in the tungsten analogue (see below) implies that this process is metal-centred. In comparison, the Mo(V)/(IV) redox potential of the bis-phenolate complex [(Tp*)Mo(O)(OC_6H_5)$_2$] is −0.88 V *vs.* Ag/AgCl in MeCN,[5] which is almost directly comparable and indicates that the biphenolate ligand is electronically similar to two separate phenolate ligands in terms of electron-donating character.

A UV/Vis/NIR spectroelectrochemical experiment was performed in acetonitrile at 243 K, and the metal-based processes were investigated; the results are shown in Fig. 2. The electronic spectrum of [(Tp*)Mo(O)(biph)] is comparable to that observed for the bis-phenolate complexes [(Tp*)Mo(O)(OC_6H_4X)$_2$] (X = H, Me, Et, halide, CN).[5] A weak, poorly resolved shoulder at *ca.* 550 nm (not shown) may be assigned as a phenolate → Mo(V) LMCT transition. A shoulder at *ca.* 350 nm is probably also a LMCT transition; higher-energy transitions in the UV region are ascribable to ligand-centred π–π* processes. On one-electron reduction to the Mo(IV) state the phenolate → Mo(V) LMCT absorption at 550 nm collapses and is replaced by a new transition at 390 nm, tentatively assigned to a Mo(IV) → Tp* MLCT transition, and a weak transition at 800 nm ($\varepsilon \approx 100$ M^{-1} cm^{-1}; not shown) which is a d–d transition associated with the Mo(IV) centre.[6f]

The corresponding tungsten complex [(Tp*)W(O)(biph)] was also isolated as a dark green solid. In keeping with the greater kinetic inertness of a third-row metal compared to its second-row congener, the reaction time for the formation of this complex was longer (16 h) and the yield much lower (6%). The FAB mass spectrum displayed a cluster of peaks with the correct isotopic pattern at m/z 681 (M^+). Infra-red spectroscopy showed the bands associated with the B–H (2556 cm^{-1}), pyrazolyl (1544 cm^{-1}) and W=O (947 cm^{-1}) vibrations. As with the molybdenum analogue, the ν(W=O) was affected on replacement of two chloride ligands by one biphenolate, shifting to lower energy (from 972 to 947 cm^{-1}) for the reasons discussed above.

X-Ray quality crystals of [(Tp*)W(O)(biph)] were grown by slow diffusion of pentane into a concentrated solution of the complex in $CHCl_3$. The crystal structure is shown in Fig. 3 (see also Table 2). The structure is very similar to that of the molybdenum analogue, with the most notable feature being the long W–N bond *trans* to the π-donor oxo ligand; other bond distances in the coordination sphere are similar to those seen for related complexes.[6a] The torsion angle between the two phenyl rings of the biphenolate ligand is 48.0°.

Fluid solution and frozen glass EPR spectra of [(Tp*)W(O)(biph)] are shown in Fig. 4. The isotropic solution EPR spectrum shows a resonance at $g_{av} = 1.776$, the expected satellites from the coupling to the tungsten isotope ^{183}W (natural abundance 14.3%, $I = 1/2$) being just observable as shoulders. The spectrum in a frozen glass at 100 K is rhombic with three clearly separated components arising from the low

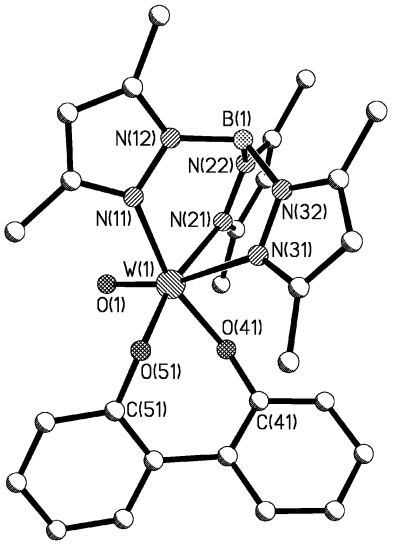

Fig. 3 Molecular structure of [(Tp*)W(O)(biph)].

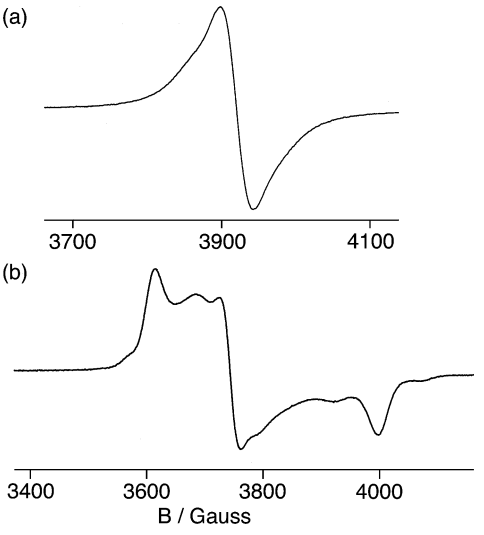

Fig. 4 X-Band EPR spectra of [(Tp*)W(O)(biph)] in (a) fluid solution and (b) a frozen glass at 100 K (1:1 dichloromethane/dichloroethane solvent in both cases).

molecular symmetry. The g values of the three components are g_1 1.859, g_2 1.794 and g_3 1.680 and the average g value is g_{av} 1.778, in good agreement with the solution spectrum. Satellites arising from coupling to ^{183}W are just visible on all three components, with approximate A values of 45, 110 and 150 G associated with g_1, g_2 and g_3 respectively; from the average of these we get $A_{iso} \approx 100$ G for the poorly-resolved coupling in Fig. 4a. The properties of this spectrum are consistent with the rather small number of other spectra of W(V) complexes in the literature.[6a,9]

The cyclic voltammogram of [(Tp*)W(O)(biph)] displays a reversible process at $E_{1/2} = -1.96$ V *vs.* $FeCp_2^{0/+}$ ($\Delta E_p =$ 96 mV) which is assigned to the metal-based W(IV)/(V) couple. This metal-based couple occurs at a potential *ca.* 580 mV more negative than the Mo(IV)/Mo(V) couple in [(Tp*)Mo(O)(biph)], reflecting the expected greater ease of oxidation of the third row metal ion. In the pair of complexes [(Tp*)MOCl(OPh)] (M = Mo, W) for example, the W(IV)/W(V) couple occurs at a potential 540 mV more negative than the Mo(IV)/Mo(V) couple.[6a]

Table 2 Selected bond distances (Å) and angles (°) for [(Tp*)W(O)(biph)]

W(1)–O(1)	1.716(4)
W(1)–O(41)	1.948(4)
W(1)–O(51)	1.972(4)
W(1)–N(11)	2.142(5)
W(1)–N(21)	2.168(4)
W(1)–N(31)	2.372(5)
O(1)–W(1)–O(41)	104.90(19)
O(1)–W(1)–O(51)	100.20(17)
O(41)–W(1)–O(51)	87.78(17)
O(1)–W(1)–N(11)	89.91(19)
O(41)–W(1)–N(11)	163.17(17)
O(51)–W(1)–N(11)	97.60(17)
O(1)–W(1)–N(21)	92.86(19)
O(41)–W(1)–N(21)	84.82(18)
O(51)–W(1)–N(21)	166.29(17)
N(11)–W(1)–N(21)	86.50(18)
O(1)–W(1)–N(31)	165.34(18)
O(41)–W(1)–N(31)	88.04(17)
O(51)–W(1)–N(31)	86.94(16)
N(11)–W(1)–N(31)	76.39(17)
N(21)–W(1)–N(31)	81.30(17)
C(41)–O(41)–W(1)	133.0(4)
C(51)–O(51)–W(1)	122.9(4)

[(Tp*)W(O)(biph)] also undergoes an irreversible process at $E_{1/2} = +0.11$ V *vs.* $FeCp_2^{0/+}$. If this were ligand (biphenolate) based it would be expected to occur at a comparable potential in [(Tp*)Mo(O)(biph)]; however the fact that this process occurs at a potential several hundred mV more negative in the tungsten complex implies that it is a metal-based W(V)/W(VI) couple. Given the very small amount of material available, and the high negative potential of the only reversible process, a spectroelectrochemical analysis was not attempted for this compound.

Tungsten(VI) complexes

In 1986 Rothwell *et al.* reported the synthesis of several tungsten(VI) aryloxides including $[Cl_2W(biph)_2]$ and $[W(biph)_3]$.[4] The latter complex $[W(biph)_3]$ displayed two reversible reduction waves at $E_{1/2} = -0.56$ and -1.56 V *vs.* Ag wire that were assigned to metal-based W(VI)/(V) and W(V)/(IV) processes; also evident is a broad oxidation wave that corresponded to the oxidation of the 2,2′-biphenol. The dichloride complexes were reported to give broad irreversible waves in the cyclic voltammograms. Following our general interest in the redox and spectroscopic properties of tungsten complexes[6a] we have re-investigated these complexes of 2,2′-biphenol.

$[W(biph)_3]$ was prepared following the literature procedure but using toluene as an alternative solvent to benzene due to the toxic nature of benzene. The EI mass spectrum shows a cluster of peaks with the correct isotope pattern at m/z 736 corresponding to M^+. The crystal structure was obtained and is shown in Fig. 5 (see also Table 3). There are two crystallographically independent but similar molecules in the structure with each having twofold symmetry, such that there are two independent half-molecules in the asymmetric unit. In each independent complex the three chelating biphenolate ligands bound to each W(VI) centre have their torsional twist in the same sense; the coordination geometry about the metal is best described as pseudo-octahedral, although a distortion towards trigonal prismatic geometry is evident (Fig. 5). In contrast, the related molybdenum and tungsten tris-catecholate complexes have dimeric structures such as $[M_2(Cl_4cat)_6]$,[10] and the neutral Mo and W tris-dithiolenes have exactly trigonal prismatic structures.[11] The W–O distances of $[W(biph)_3]$ span the range 1.893(3) to 1.906(3) Å; the C–O bond distances of *ca.* 1.38 Å are characteristic of a single bond. The torsion angles of the biphenolate ligands about W(1) are 42.0° and 46.0°, and about W(2) are 45.3° and 46.8°.

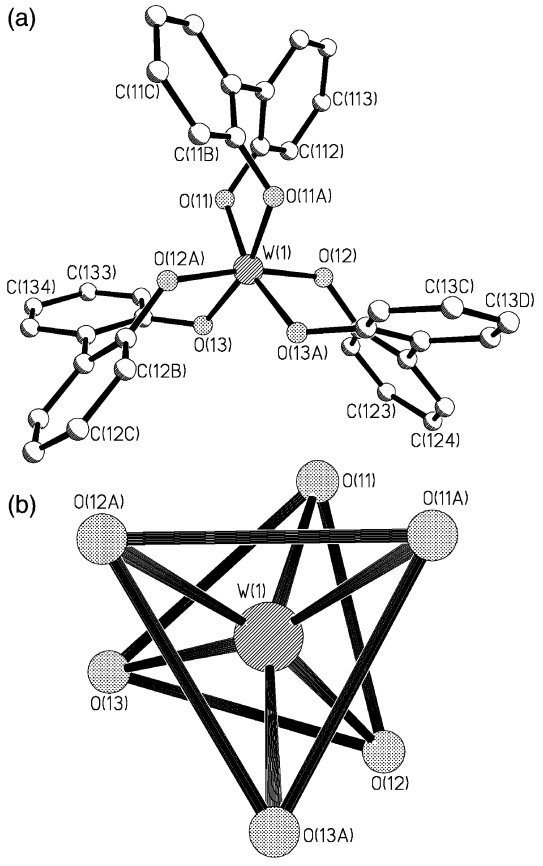

Fig. 5 (a) Molecular structure of $[W(biph)_3]$, and (b) a view of the coordination sphere emphasising the distortion towards trigonal prismatic geometry. Only one of the crystallographically independent complex units is shown; the other is similar.

The cyclic voltammogram of $[W(biph)_3]$ recorded in CH_2Cl_2 [Fig. 6(a)] shows two chemically reversible processes, which correspond to the W(V)/(VI) couple at $E_{1/2} = -0.97$ V *vs.* $FeCp_2^{0/+}$ (ΔE_p 122 mV), and the W(IV)/(V) couple at $E_{1/2} = -2.04$ V *vs.* $FeCp_2^{0/+}$ (ΔE_p 130 mV), in agreement with the literature.[4] A UV/Vis/NIR spectroelectrochemical experiment was carried out in CH_2Cl_2 at 243 K and the results are shown in Fig. 7. The spectrum of the complex in its initial W(VI) state exhibits a band at 275 nm which is assigned to a π–π* ligand-centred transition, and a much broader absorption with

Table 3 Selected bond distances (Å) and angles (°) for $[W(biph)_3]$

W(1)–O(13)	1.899(3)	W(2)–O(23)	1.893(3)
W(1)–O(12)	1.902(3)	W(2)–O(21)	1.900(3)
W(1)–O(11)	1.906(3)	W(2)–O(22)	1.905(3)
O(11)–C(111)	1.384(5)	O(21)–C(211)	1.369(5)
O(12)–C(121)	1.378(5)	O(22)–C(221)	1.389(5)
O(13)–C(131)	1.387(5)	O(23)–C(231)	1.375(5)
O(13A)–W(1)–O(13)	102.84(18)	O(23A)–W(2)–O(23)	84.40(17)
O(13A)–W(1)–O(12)	82.85(12)	O(22A)–W(2)–O(22)	167.61(17)
O(13)–W(1)–O(12)	89.93(12)	O(23A)–W(2)–O(21)	172.23(11)
O(12A)–W(1)–O(12)	168.44(17)	O(23)–W(2)–O(21)	89.93(12)
O(13A)–W(1)–O(11)	164.43(12)	O(21A)–W(2)–O(21)	96.18(17)
O(13)–W(1)–O(11)	88.33(12)	O(23)–W(2)–O(22A)	98.10(12)
O(12A)–W(1)–O(11)	102.34(12)	O(21)–W(2)–O(22A)	84.44(12)
O(12)–W(1)–O(11)	86.39(12)	O(23A)–W(2)–O(22)	98.10(12)
O(13)–W(1)–O(11A)	164.43(11)	O(23)–W(2)–O(22)	91.08(12)
O(12)–W(1)–O(11A)	102.34(12)	O(21A)–W(2)–O(22)	84.44(12)
O(11)–W(1)–O(11A)	82.99(17)	O(21)–W(2)–O(22)	87.30(12)
C(111)–O(11)–W(1)	128.7(3)	C(211)–O(21)–W(2)	135.5(3)
C(121)–O(12)–W(1)	132.8(3)	C(221)–O(22)–W(2)	128.0(3)
C(131)–O(13)–W(1)	128.9(3)	C(231)–O(23)–W(2)	134.5(3)

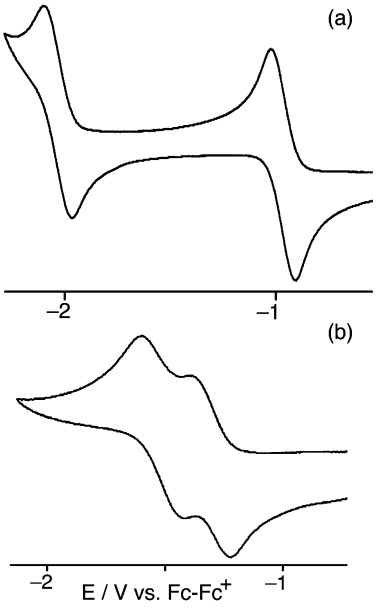

Fig. 6 Cyclic voltammograms of (a) $[W(biph)_3]$, and (b) $[Cl_6W_2(biph)_3]$ (both in CH_2Cl_2 using a Pt-disk working electrode).

a long low-energy tail, centred at 377 nm, which we assign to a phenolate → W(VI) LMCT transition. On one-electron reduction to the W(V) state, the LMCT transition mostly collapses but the LC transition remains virtually unchanged, in agreement with these assignments. A shoulder at *ca.* 330 nm may be assigned as a phenolate → W(V) LMCT (higher in energy and less intense than the LMCT involving the W(VI) centre, as expected), and a very weak transition at 535 nm (ε *ca.* 50 M^{-1} cm^{-1}) is likely to be a d–d transition associated with the d^1 metal centre. Upon a further one-electron reduction to the W(IV) state, the phenolate → W(V) LMCT transition disappears and the LC transition is shifted to slightly lower energy slightly. Two weak new transitions appear at 430 nm (ε 800 M^{-1} cm^{-1}) and *ca.* 600 nm (shoulder). The nature of these is not obvious but one of them at least can be assigned as a d–d transition associated with the W(IV) centre.

We also attempted to repeat the synthesis of $[Cl_2W(biph)_2]$, again replacing benzene with toluene. Under these conditions we found no evidence for formation of mononuclear $[Cl_2W(biph)_2]$; instead the product of the reaction was the bridged dinuclear complex $[Cl_6W_2(biph)_3]$, as shown by the FAB mass spectrum which contained clusters of peaks with the correct isotope patterns at m/z 1155 $(M + Na^+)$, 1134 (M^+) and 1098 $(M - Cl)^+$.

X-Ray quality crystals of $[Cl_6W_2(biph)_3]$ were grown from $CHCl_3$/heptane as dark red plates. The crystal structure of the complex molecules is shown in Fig. 8 (see also Table 4).

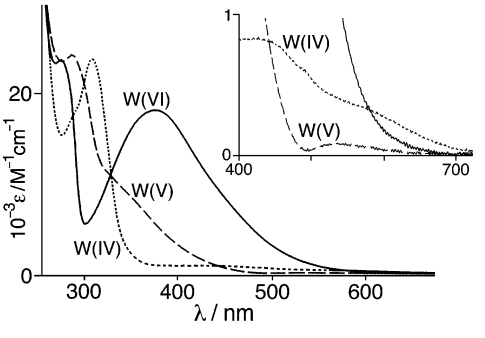

Fig. 7 Electronic spectra of $[W(biph)_3]^{n-}$ ($n = 0$, solid line; 1, dashed line, 2, dotted line) from an OTTLE experiment in CH_2Cl_2 at 243 K.

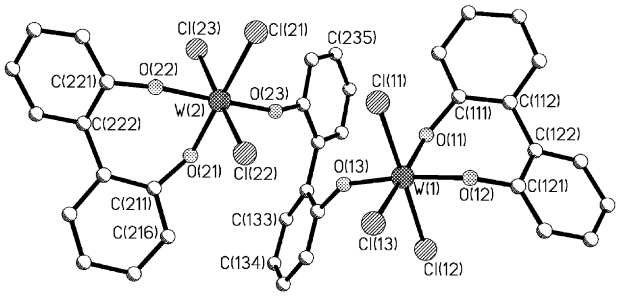

Fig. 8 Molecular structure of $[Cl_6W_2(biph)_3]$.

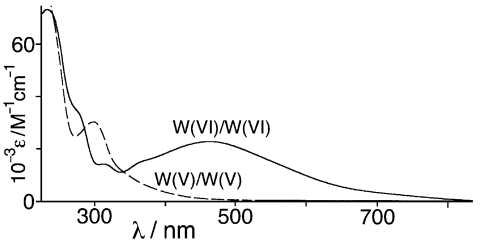

Fig. 9 Electronic spectra of $[Cl_6W_2(biph)_3]^{n-}$ ($n = 0$, solid line; $n = 2$, dashed line) from an OTTLE experiment in CH_2Cl_2 at 243 K.

The structure contains two {$Cl_3W(biph)$} units which are connected by an additional bridging biphenolate ligand; accordingly the complex contains biphenolate in two different coordination modes, with the metal centres both having a distorted octahedral *mer*-O_3Cl_3 coordination environment. The W–O bond distances for the bridging biphenolate ligand and the terminal biphenolate ligands are very similar, being on average 1.85 Å and 1.86 Å respectively, slightly shorter than in $[W(biph)_3]$ (1.90 Å). The torsion angles within the biphenolate ligands are 43.9° and 38.4° for the terminal ligands, whereas the twist of the bridging biphenolate is much greater at 55.1°. The W···W separation is 5.32 Å.

Rothwell mentioned the presence of a dimeric tungsten species, $[W_2(Mecat)_6]$ (Mecat = 4-methylcatecholate), in the analogous reaction to form $[W(Mecat)_3]$; this dimer was reported to be stable in both solid and solution states. An important factor controlling formation of the bridged dinuclear species is the steric bulk of the substituent on the catecholate ligands: those with sterically demanding substituents, such as 3,5-di-*tert*-butylcatecholate, were not able to form the bridged dinuclear species, whilst those with less bulky groups such as 4-methylcatecholate were more likely to act as bridging ligands.[4] Pierpont *et al.* had previously reported that the related $[M_2(O_2C_6Cl_4)_6]$ complexes (M = Mo, W) were dimeric in only the solid state with the pseudo-octahedral metal centres being bridged by two catecholate ligands.[10] Since biphenolate has a greater capacity to act as a bridging ligand than catecholate, because of the possibility of twisting about the central C–C bond to allow the phenolate donors to point in different directions, the formation of the bridged species $[Cl_6W_2(biph)_3]$ is not unexpected.

Table 4 Selected bond distances (Å) and angles (°) for $[Cl_6W_2(biph)_3]$

W(1)–O(13)	1.853(4)	W(2)–O(23)	1.847(4)
W(1)–O(12)	1.854(4)	W(2)–O(22)	1.871(5)
W(1)–O(11)	1.878(4)	W(2)–O(21)	1.872(5)
W(1)–Cl(11)	2.3189(19)	W(2)–Cl(21)	2.331(2)
W(1)–Cl(13)	2.3388(17)	W(2)–Cl(22)	2.3308(18)
W(1)–Cl(12)	2.3426(19)	W(2)–Cl(23)	2.3366(18)
O(11)–C(111)	1.375(8)	O(21)–C(211)	1.345(8)
O(12)–C(121)	1.389(8)	O(22)–C(221)	1.359(8)
O(13)–C(131)	1.380(8)	O(23)–C(231)	1.367(7)
O(13)–W(1)–O(12)	168.5(2)	O(23)–W(2)–O(22)	171.78(19)
O(13)–W(1)–O(11)	90.76(19)	O(23)–W(2)–O(21)	90.7(2)
O(12)–W(1)–O(11)	86.05(18)	O(22)–W(2)–O(21)	86.4(2)
O(13)–W(1)–Cl(11)	95.05(15)	O(23)–W(2)–Cl(21)	92.46(16)
O(12)–W(1)–Cl(11)	95.75(15)	O(22)–W(2)–Cl(21)	91.11(15)
O(11)–W(1)–Cl(11)	85.47(15)	O(21)–W(2)–Cl(21)	174.42(15)
O(13)–W(1)–Cl(13)	94.15(14)	O(23)–W(2)–Cl(22)	94.68(14)
O(12)–W(1)–Cl(13)	90.57(14)	O(22)–W(2)–Cl(22)	92.86(14)
O(11)–W(1)–Cl(13)	170.91(15)	O(21)–W(2)–Cl(22)	87.39(16)
Cl(11)–W(1)–Cl(13)	86.47(7)	Cl(21)–W(2)–Cl(22)	87.77(7)
O(13)–W(1)–Cl(12)	84.73(15)	O(23)–W(2)–Cl(23)	86.43(14)
O(12)–W(1)–Cl(12)	84.60(15)	O(22)–W(2)–Cl(23)	86.18(14)
O(11)–W(1)–Cl(12)	96.17(15)	O(21)–W(2)–Cl(23)	95.09(16)
Cl(11)–W(1)–Cl(12)	178.35(7)	Cl(21)–W(2)–Cl(23)	89.69(8)
Cl(13)–W(1)–Cl(12)	91.91(7)	Cl(22)–W(2)–Cl(23)	177.27(8)
C(111)–O(11)–W(1)	134.0(4)	C(211)–O(21)–W(2)	140.4(4)
C(121)–O(12)–W(1)	137.2(4)	C(221)–O(22)–W(2)	138.9(4)
C(131)–O(13)–W(1)	147.6(4)	C(231)–O(23)–W(2)	154.1(4)

The cyclic voltammogram of $[Cl_6W_2(biph)_3]$ was recorded in dichloromethane and is shown in Fig. 6(b). Four redox processes are apparent. The two closely-spaced chemically reversible processes at $E_{1/2} = -1.51$ V ($\Delta E_p = 125$ mV) and −1.34 V ($\Delta E_p = 133$ mV) *vs.* $FeCp_2^{0/+}$ are assigned as the successive metal-based W(VI)/(V) couples. The separation of 170 mV between these two metal-based redox processes indicates a weak electronic interaction between them,[12] which was investigated by UV/Vis/NIR spectroelectrochemistry (see below). The remaining two processes at $E_{1/2} = -0.36$ V *vs.* $FeCp_2^{0/+}$ and −0.05 V *vs.* $FeCp_2^{0/+}$ are irreversible and, given the +6 oxidation state of the tungsten centres, are necessarily assigned as ligand-based oxidations.

The UV/Vis/NIR spectroelectrochemical properties of $[Cl_6W_2(biph)_3]$ in CH_2Cl_2 at 243 K are shown in Fig. 9. By analogy with the electronic spectrum of $[W(biph)_3]$, the band at 480 nm can be assigned to a phenolate → W(VI) LMCT transition. On successive one-electron reductions to the W(V)/W(VI) mixed-valence state and then the W(V)/W(V) isovalent states, this LMCT transition steadily collapses to leave the ligand-centred transition in the UV region as the only significant feature of the spectrum, although a broad shoulder on the low-energy side of this at *ca.* 350 nm is indicative of residual LMCT associated with the W(V) centre.

Despite the indication of an electronic interaction between the metal centres from the electrochemical data, we found no evidence for an inter-valence charge-transfer transition in the mono-reduced form of $[Cl_6W_2(biph)_3]$, presumably because of the highly twisted nature of the bridging ligand which will preclude the orbital delocalisation pathway necessary for the electron transfer. Accordingly the separation between the successive W(V)/W(VI) couples can be ascribed to a through-space electrostatic effect rather than to any delocalisation of the unpaired electron in the mixed-valence state.[12]

[(bpy)$_2$Ru(biph)]

The complex [(bpy)$_2$Ru(biph)] was prepared by refluxing [(bpy)$_2$RuCl$_2$] with 2,2′-biphenol in ethanol in the presence of base for 4 hours. On addition of base the colour of the solution changed from the dark red of [(bpy)$_2$RuCl$_2$] to blue. Once the reaction had gone to completion the reaction volume was reduced and the crude product was purified by column chromatography (Sephadex LH20, eluting with CH_3OH). The product eluted as a blue band, whose FAB mass spectrum displayed a peak cluster at m/z 598 with the correct isotopic pattern. It is noteworthy that this complex has the same donor set as $[Ru(hpb)_2]^+$ [where Hhpb is the terdentate bipyridine-phenol ligand 6-(2-hydroxyphenyl)-2,2′-bipyridine].[13]

X-Ray quality crystals were obtained as dark red blocks from slow diffusion of $^iPr_2O$ into a CH_2Cl_2 solution of the complex. The structure is displayed in Fig. 10 (see also Table 5). The coordination geometry at the metal centre is

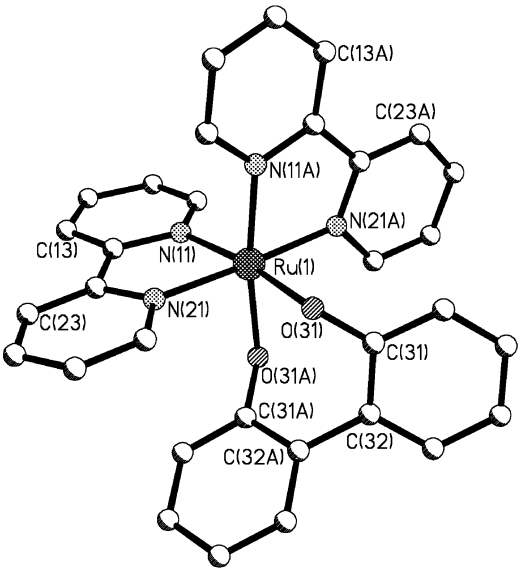

Fig. 10 Molecular structure of the metal complex component of $[(bpy)_2Ru(biph)]\cdot 2CH_2Cl_2$.

distorted octahedral, with the complex having twofold symmetry. The Ru–O bond length of 2.0774(18) Å and the Ru–N distances are comparable to those of numerous other $\{(bpy)_2Ru^{II}\}$-based complexes. The Ru(1)–N(11) distance of 2.017(2) Å is slightly shorter than the Ru(1)–N(21) distance of 2.037(2) Å as it is *trans* to the phenolate unit, whose σ-donating character increases the electron density at the metal centre which in turn increases the Ru(dπ)–bpy(π*) back bonding on that axis. A similar effect has been seen in another Ru(II) complexes with a mixed pyridine/phenolate donor set.[14] The torsion angle between the two phenyl rings of the biphenolate ligand is 58.5°.

The cyclic voltammogram of $[Ru(bpy)_2(biph)]$ was recorded in acetonitrile and displayed three processes. A reversible oxidation at $E_{1/2} = -0.50$ V *vs.* $FeCp_2^{0/+}$ (ΔE_p 68 mV) is assigned as a Ru(II)/Ru(III) couple. Also observed are a poorly defined reduction at $E_{1/2} = -2.14$ V *vs.* $FeCp_2^{0/+}$ and an irreversible oxidation at $E_{1/2} = +0.56$ V *vs.* $FeCp_2^{0/+}$. The reductive process is assigned as bpy-based couple whilst the second oxidation could be either ligand-based (irreversible oxidations associated with phenolate ligands have been observed in related complexes) or a metal-based Ru(III)/Ru(IV) couple. For comparison, the Ru(II)/Ru(III) redox potential in the related mononuclear complex $[Ru(hpb)_2]^+$, having four pyridyl

Table 5 Selected bond lengths (Å) and angles (°) of $[(bpy)_2Ru(biph)]$

Ru(1)–N(11)	2.017(2)
Ru(1)–N(21)	2.037(2)
Ru(1)–O(31)	2.0774(18)
O(31)–C(31)	1.338(3)
N(11)–Ru(1)–N(11A)	93.09(12)
N(11)–Ru(1)–N(21A)	99.20(8)
N(11)–Ru(1)–N(21)	78.84(8)
N(11A)–Ru(1)–N(21)	99.20(8)
N(21A)–Ru(1)–N(21)	177.19(11)
N(11)–Ru(1)–O(31)	171.08(7)
N(11A)–Ru(1)–O(31)	89.73(8)
N(21A)–Ru(1)–O(31)	89.65(8)
N(21)–Ru(1)–O(31)	92.36(8)
N(11)–Ru(1)–O(31A)	89.73(8)
N(21)–Ru(1)–O(31A)	89.65(8)
O(31)–Ru(1)–O(31A)	88.76(10)
C(31)–O(31)–Ru(1)	117.19(15)
C(16)–N(11)–Ru(1)	125.74(18)
C(12)–N(11)–Ru(1)	116.74(17)

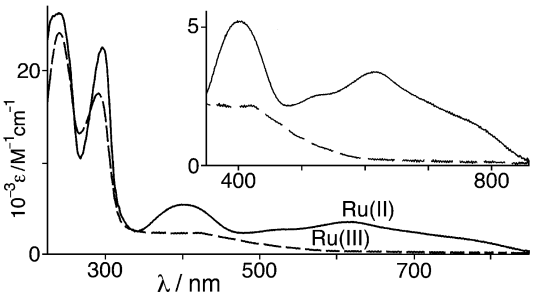

Fig. 11 Electronic spectra of $[(bpy)_2Ru(biph)]^{n+}$ ($n = 0$, solid line; $n = 1$, dashed line) from an OTTLE experiment in MeCN at 243 K (inset: expansion of the visible region).

and two *cis*-phenolate donors, is −0.51 V *vs.* $FeCp_2^{0/+}$ in MeCN,[13] confirming again that the biphenolate ligand is electronically comparable to two independent phenolate ligands.

The electronic spectrum of $[(bpy)_2Ru(biph)]$ in acetonitrile (Fig. 11) shows two intense bands at 237 and 294 nm ($\varepsilon \approx$ 26 000 and 22 200 dm^3 mol^{-1} cm^{-1} respectively) which are assigned to Ru(II) → π*(bpy) MLCT and π–π*(bpy) LC transitions respectively. Two bands of moderate intensity at 397 and 610 nm are assigned to Ru(II) → π*(bpy) MLCT transitions, with the wide range of these caused by the low symmetry of the ligand field. This spectrum is similar to that of $[(bpy)_2Ru(\mu\text{-}OR)_2Ru(bpy)_2]^{2+}$ (R = Me, Et) in which the metal centres have a comparable coordination environment.[15] On one-electron oxidation to $[(bpy)_2Ru(biph)]^+$ the transition at 397 nm diminishes considerably in intensity, and the transition at 610 nm collapses completely, in agreement with their MLCT character. There is however no evidence for appearance of a low-energy phenolate → Ru(III) LMCT transition which might be expected by comparison with related complexes.[13]

Experimental

General details

2,2′-Biphenol was purchased from Sigma-Aldrich, and WCl_6 was purchased from Acros. The metal reagents $[(Tp^*)OMoCl_2]$,[5] $[(Tp^*)OWCl_2]$[6a,16] and $[(bpy)_2RuCl_2]\cdot 2H_2O$[17] were prepared following literature procedures. Instrumentation used for routine characterisation, and electrochemical and UV/Vis/NIR spectro-electrochemical studies, has been described in previous papers.[6,18] FAB mass spectra were recorded at the EPSRC National Mass Spectrometry Service Centre, at the University of Wales Swansea. X-Band EPR spectra were recorded on a Bruker ESP-300E instrument.

Preparations

$[W(biph)_3]$. This synthesis is a minor variation of a published method.[4] 2,2′-Biphenol (0.5 g, 2.68 mmol) and WCl_6 (0.35 g, 0.89 mmol) were stirred together *in vacuo* for 3 h. Dry toluene (25 cm^3) was then added, and the reaction mixture was heated at reflux under N_2 for 6 h. The solvent was then removed to give a brown/red solid, which was heated *in vacuo* at 100 °C for 1 h. The solid was then recrystallised from $CHCl_3$/hexane to yield X-ray quality crystals of the product (100 mg, 15%). EIMS: m/z 736 (M^+). Found: C, 57.9; H, 3.5%. Required for $C_{36}H_{24}O_6W$: C, 58.7; H 3.3%.

$[Cl_6W_2(biph)_3]$. WCl_6 (0.53 g, 1.34 mmol) and 2,2′-biphenol (0.5 g, 2.68 mmol) were stirred together under N_2 for 2 h. Dry toluene (20 cm^3) was added, and a stream of N_2 gas was blown over the reaction mixture at room temperature for 8 h (to remove evolved HCl). The solvent was removed and the brown solid was purified by column chromatography (flash silica,

Table 6 Crystallographic data[a]

Compound	[(Tp*)Mo(O)(biph)]	[(Tp*)W(O)(biph)]	[W(biph)$_3$]	[Cl$_6$W$_2$(biph)$_3$]	[(bpy)$_2$Ru(biph)]·2CH$_2$Cl$_2$
Empirical formula	$C_{27}H_{30}BMoN_6O_3$	$C_{27}H_{30}BN_6O_3W$	$C_{36}H_{24}O_6W$	$C_{36}H_{24}Cl_6O_6W_2$	$C_{34}H_{28}Cl_4N_4O_2Ru$
Formula weight	593.32	681.23	736.40	1132.95	767.48
System, space group	Monoclinic, $P2_1/c$	Monoclinic, $P2_1/c$	Orthorhombic, $Pccn$	Monoclinic, $P2(1)/n$	Monoclinic, $C2/c$
a/Å	12.848(2)	15.410(3)	16.8678(12)	9.985(2)	13.467(5)
b/Å	9.7316(14)	10.0634(18)	17.776(2)	22.734(5)	15.593(6)
c/Å	21.776(5)	17.134(4)	19.036(2)	16.038(3)	15.861(6)
β/deg	106.361(17)	105.629(11)	90	93.85(2)	98.310(7)
V/Å^3	2612.5(8)	2558.9(9)	5707.8(10)	3632.2(12)	3296(2)
Z	4	4	8	4	4
Calcd density/ Mg m^{-3}	1.509	1.768	1.714	2.072	1.547
Data, restraints, parameters	5998, 0, 352	5852, 0, 347	3727, 0, 389	8307, 0, 451	3779, 0, 214
μ(mm^{-1})	0.544	4.557	4.096	6.816	0.838
$R1$ [$I > 2\sigma(I)$], $wR2$[a]	0.0380, 0.0887	0.0448, 0.1088	0.0207, 0.0515	0.0400, 0.0736	0.0373, 0.0983

[a] The value of $R1$ is based on selected data with $I > 2\sigma(I)$; the value of $wR2$ is based on all data. Data in common: Bruker-AXS SMART diffractometer with Mo-Kα radiation; T = 173 K.

eluting with CH_2Cl_2:hexane, 2:1) to yield the product (250 mg, 32%). FABMS: m/z 1155 (M + Na)$^+$, 1134 (M$^+$) and 1098 (M − Cl)$^+$. ^{1}H NMR (270 MHz, $CDCl_3$): δ 7.73 (2H, d, J 7.8), 7.65–7.59 (4H, m), 7.58–7.45 (6H, m), 7.35 (2H, td, J 7.7, 1.6), 7.27–7.19 (2H, m), 7.12–6.98 (6H, m), 6.34 (2H, dd, J 8.3, 1.1 Hz). Found: C, 38.4; H, 1.9%. Required for $C_{36}H_{24}O_6Cl_6W_2$: C, 38.2; H 2.1%.

[(Tp*)Mo(O)(biph)]. [(Tp*)Mo(O)Cl$_2$] and 2,2′-biphenol were dried under vacuum for several hours before use. Pyridine was dried over molecular sieves and degassed for 20 minutes before use.

To a stirred solution of 2,2′-biphenol (50 mg, 0.27 mmol) in pyridine (25 cm^3) was added sodium hydride (13 mg, 0.54 mmol). The mixture was heated at reflux for 1 h. On cooling, [(Tp*)Mo(O)Cl$_2$] (130 mg, 0.27 mmol) was added to the solution, and a colour change was observed from green to orange after several minutes. The solution was then heated at reflux for 2 h. The solvent was removed to give an orange residue which was purified by column chromatography (flash silica, eluting with CH_2Cl_2) to yield the product as a green/yellow solid (68 mg, 42%). EIMS: m/z 595 (M$^+$), 498 (M$^+$ − pyrazolyl ring). IR (solid state): 2923 cm^{-1} (C–H), 2541 cm^{-1} (B–H), 1543 cm^{-1} (pyrazolyl ring), 1203 cm^{-1} (C–O), 941 cm^{-1} (Mo=O). Found: C, 55.4; H, 5.5; N, 13.8%. Required for $C_{27}H_{30}N_6O_3BMo$: C, 54.7; H, 5.1; N, 14.2%.

[(Tp*)W(O)(biph)]. [(Tp*)W(O)Cl$_2$] and 2,2′-biphenol were dried under vacuum for several hours before use. Pyridine was dried over molecular sieves and degassed for 20 minutes before use.

To a stirred solution of 2,2′-biphenol (50 mg, 0.27 mmol) in pyridine (20 cm^3) was added sodium hydride (13 mg, 0.54 mmol). The mixture was heated at reflux for 1 h. On cooling [(Tp*)W(O)Cl$_2$] (152 mg, 0.27 mmol) was added to the solution, and the reaction mixture was then heated at reflux for 16 h, during which time the solution colour changed from blue to purple and eventually green. Evaporation of the pyridine gave a green solid that was purified by column chromatography (flash silica, eluting with CH_2Cl_2). The product was isolated as a green solid (11 mg, 6%). EIMS: m/z 681 (M$^+$). IR (CH_2Cl_2 solution): 2556 cm^{-1} (BH), 1544 cm^{-1} (pyrazolyl), 947 cm^{-1} (W=O). Found: C, 47.9; H, 4.8; N, 12.3%. Required for $C_{27}H_{30}N_6O_3BW$: C, 47.6; H 4.4; N, 12.3%.

[(bpy)$_2$Ru(biph)]. To a solution of [(bpy)$_2$RuCl$_2$]·2H$_2$O (140 mg, 0.27 mmol) in ethanol (10 cm^3) was added a solution of $AgNO_3$ (91 mg, 0.54 mmol) in water (5 cm^3). The solution was refluxed for 0.5 h. On cooling the precipitated AgCl was filtered through celite, and the deep red filtrate (containing [Ru(bpy)$_2$(H$_2$O)$_2$]$^{2+}$) was then reduced in volume to *ca.* 20 cm^3. To the filtrate was added 2,2′-biphenol (50 mg, 0.27 mmol) and the reaction was heated; once reflux temperature had been achieved NaOH (aq) was added and the solution immediately changed to a deep blue colour. Heating at reflux was continued for 2 h. On cooling the reaction volume was reduced (to *ca.* 3 cm^3) and purified by column chromatography on Sephadex-LH20, eluting with MeOH. The product eluted as the blue second band; removal of the solvent gave the product as a purple solid (116 mg, 72%). FAB MS: m/z 598 (M$^+$), 414 (M$^+$ − biph).

^{1}H NMR (270 MHz, $CDCl_3$): δ 9.25 (2H, br s), 8.14 (2H, d, J 7.4), 8.06 (2H, d, J 8.4; bpy), 7.72 (2H, t, J 7.4), 7.25 (8H, m), 6.90 (2H, br s), 6.52 (2H, t, J 7.2); 6.43 (2H, t, J 7.5), 5.36 (2H, d, J 7.5 Hz). Found: C, 63.9; H, 4.2; N, 9.3%. Required for $C_{32}H_{24}N_4O_2Ru$: C, 64.3; H 4.0; N, 9.4%.

X-Ray crystallography

For each complex a suitable crystal was coated with hydrocarbon oil and attached to the tip of a glass fibre, which was then transferred to a Bruker-AXS SMART diffractometer under a stream of cold N$_2$ at 173 K. Details of the crystal parameters, data collection and refinement for each of the structures are collected in Table 6. After data collection, in each case an empirical absorption correction (SADABS) was applied,[19] and the structures were then solved by conventional direct methods and refined on all F^2 data using the SHELX suite of programs.[20] In all cases (except one, below), non-hydrogen atoms were refined with anisotropic thermal parameters; hydrogen atoms were included in calculated positions and refined with isotropic thermal parameters which were *ca.* 1.2× (aromatic CH) or 1.5× (Me) the equivalent isotropic thermal parameters of their parent carbon atoms. For the structure of [(Tp*)W(O)(biph)], one of the atoms [N(12)] was refined isotropically to prevent it from becoming 'non-positive-definite' when anisotropic thermal parameters were used.†

† CCDC reference numbers 199480–199484. See http://www.rsc.org/suppdata/nj/b2/b211997h/ for crystallographic data in .cif or other electronic format.

Acknowledgements

We thank the EPSRC for financial support, and Dr. John Maher and Miss Keira Stobie for assistance with the EPR spectroscopy.

References

1 L. Pu, *Chem. Rev.*, 1998, **98**, 2405.
2 (*a*) A. Kayal and S. C. Lee, *Inorg. Chem.*, 2002, **41**, 321 and references therein; (*b*) B. Antelmann, M. H. Chisholm, S. S. Iyer, J. C. Huffman, D. Navarro-Llobet, M. Pagel, W. J. Simonsick and W. Q. Zhong, *Macromolecules*, 2001, **34**, 3159; (*c*) A. Vanderlinden, C. J. Schaverien, N. Maijboom, C. Ganter and A. G. Orpen, *J. Am. Chem. Soc.*, 1995, **117**, 3008.
3 (*a*) K. Thiele, H. Görls, W. Imhof and W. Siedel, *Z. Anorg. Allg. Chem.*, 2002, **628**, 107; (*b*) A. R. Schake, E. A. Schmitt, A. J. Conti, W. E. Streib, J. C. Huffman, D. N. Hendrickson and G. Christou, *Inorg. Chem.*, 1991, **30**, 3192.
4 S. M. Beshouri and I. P. Rothwell, *Inorg. Chem.*, 1986, **25**, 1962.
5 W. E. Cleland, Jr., K. M. Barhhart, K. Yamanouchi, D. Collison, F. E. Mabbs, R. B. Ortega and J. H. Enemark, *Inorg. Chem.*, 1987, **26**, 1017.
6 (*a*) K. E. Stobie, Z. R. Bell, T. W. Munhoven, J. P. Maher, J. A. McCleverty, M. D. Ward, E. J. L. McInnes, F. Totti and D. Gatteschi, *Dalton Trans.*, 2003, 36; (*b*) A. M. McDonagh, J. A. McCleverty and M. D. Ward, *New J. Chem.*, 2001, **25**, 1236; (*c*) S. R. Bayly, E. R. Humphrey, H. de Chair, C. G. Paredes, Z. R. Bell, J. C. Jeffery, J. A. McCleverty, M. D. Ward, F. Totti, D. Gatteschi, S. Courric and C. G. Screttas, *J. Chem. Soc., Dalton Trans.*, 2001, 1401; (*d*) A. McDonagh, S. R. Bayly, D. J. Riley, M. D. Ward, J. A. McCleverty, M. A. Cowin, C. N. Morgan, R. Varrazza, R. V. Penty and I. H. White, *Chem. Mater.*, 2000, **12**, 2523; (*e*) S. Bayly, J. A. McCleverty, M. D. Ward, D. Gatteschi and F. Totti, *Inorg. Chem.*, 2000, **39**, 1288; (*f*) N. C. Harden, E. R. Humphrey, J. C. Jeffery, S.-M. Lee, M. Marcaccio, J. A. McCleverty, L. H. Rees and M. D. Ward, *J. Chem. Soc., Dalton Trans.*, 1999, 2417; (*g*) V. A. Ung, S. M. Couchman, J. C. Jeffery, J. A. McCleverty, M. D. Ward, F. Totti and D. Gatteschi, *Inorg. Chem.*, 1999, **38**, 365.
7 P. Basu, M. A. Bruck, Z. Li, I. K. Dhawan and J. H. Enemark, *Inorg. Chem.*, 1995, **34**, 405.
8 C. G. Pierpont and R. M. Buchanan, *Coord. Chem. Rev.*, 1981, **38**, 45.
9 (*a*) F. M. Horning and W. Kaim, *J. Chem. Soc., Faraday Trans.*, 1994, **90**, 2909; (*b*) C. A. Rice, P. M. H. Kroneck and J. T. Spence, *Inorg. Chem.*, 1981, **20**, 1996; (*c*) F. M. Horning, O. Heilmann, W. Kaim, S. Zalis and J. Fiedler, *Inorg. Chem.*, 2000, **39**, 4052; (*d*) E. S. Davies, G. M. Aston, R. L. Beddoes, D. Collison, A. Dinsmore, A. Docrat, J. A. Joule, C. R. Wilson and C. D. Garner, *J. Chem. Soc., Dalton Trans.*, 1998, 3647; (*e*) B. A. Goodman and J. B. Raynor, *Adv. Inorg. Chem. Radiochem.*, 1970, **13**, 135.
10 (*a*) C. G. Pierpont, H. H. Downs and T. G. Rukavina, *J. Am. Chem. Soc.*, 1974, **96**, 5573; (*b*) C. G. Pierpont and H. H. Downs, *J. Am. Chem. Soc.*, 1975, **97**, 2123.
11 (*a*) G. F. Brown and E. I. Steifel, *Inorg. Chem.*, 1973, **12**, 2140; (*b*) E. I. Steifel and G. F. Brown, *Inorg. Chem.*, 1972, **11**, 434; (*c*) R. Eisenberg, *Prog. Inorg. Chem.*, 1970, **12**, 295; (*d*) J. A. McCleverty, *Prog. Inorg. Chem.*, 1968, **10**, 145.
12 M. D. Ward, *Chem. Soc. Rev.*, 1995, **24**, 121.
13 D. A. Bardwell, D. Black, J. C. Jeffery, E. Schatz and M. D. Ward, *J. Chem. Soc., Dalton Trans.*, 1993, 2321.
14 B. M. Holligan, J. C. Jeffery, M. K. Norgett, E. Schatz and M. D. Ward, *J. Chem. Soc., Dalton Trans.*, 1992, 3345.
15 D. A. Bardwell, L. Horsburgh, J. C. Jeffery, L. F. Joulié, M. D. Ward, I. Webster and L. J. Yellowlees, *J. Chem. Soc., Dalton Trans.*, 1996, 2527.
16 C. Persson and C. Andersson, *Inorg. Chim. Acta*, 1993, **203**, 235.
17 B. P. Sullivan, D. J. Salmon and T. J. Meyer, *Inorg. Chem.*, 1978, **17**, 3334.
18 S.-M. Lee, R. Kowallick, M. Marcaccio, J. A. McCleverty and M. D. Ward, *J. Chem. Soc., Dalton Trans.*, 1998, 3443.
19 G. M. Sheldrick, SADABS, A program for absorption correction with the Siemens SMART area-detector system, University of Göttingen, 1996.
20 G. M. Sheldrick, SHELXS-97 and SHELXL-97 programs for crystal structure solution and refinement, University of Göttingen, 1997.